

## Research Article

# CO<sub>2</sub> Reforming Characteristics under Visible Light Response of Cr- or Ag-Doped TiO<sub>2</sub> Prepared by Sol-Gel and Dip-Coating Process

Akira Nishimura,<sup>1</sup> Go Mitsui,<sup>1</sup> Katsuya Nakamura,<sup>1</sup> Masafumi Hirota,<sup>1</sup> and Eric Hu<sup>2</sup>

<sup>1</sup> Division of Mechanical Engineering, Graduate School of Engineering, Mie University, 1577 Kurimamachiya-cho, Tsu 514-8507, Japan

<sup>2</sup> School of Mechanical Engineering, The University of Adelaide, Adelaide, SA 5005, Australia

Correspondence should be addressed to Akira Nishimura, nishimura@mach.mie-u.ac.jp

Received 25 May 2011; Revised 2 August 2011; Accepted 2 August 2011

Academic Editor: Jinlong Zhang

Copyright © 2012 Akira Nishimura et al. This is an open access article distributed under the Creative Commons Attribution License, which permits unrestricted use, distribution, and reproduction in any medium, provided the original work is properly cited.

A Cr- or Ag-doped TiO<sub>2</sub> film was prepared by sol-gel and dip-coating process and used as the photocatalyst for CO<sub>2</sub> reforming under the visible light. The ratio of amount of Cr or Ag added to amount of Ti in TiO<sub>2</sub> sol solution ( $R$ ) varied from 0 to 100 wt% or 0 to 50 wt%, respectively. The total layer number of Cr- or Ag-doped TiO<sub>2</sub> film ( $N$ ) coated was changed. The CO<sub>2</sub> reforming performance with the Cr- or Ag-doped TiO<sub>2</sub> film was tested under a Xe lamp with or without ultraviolet (UV) light. As a result, when  $N$  equals to 1, the concentration of CO which was a product from CO<sub>2</sub> reforming was maximized in Cr doping case for  $R = 70$  wt% and in Ag doping case for  $R = 1$  wt%, respectively. The best result of concentration of CO = 8306 ppmV, concentration of CH<sub>4</sub> = 1367 ppmV, concentration of C<sub>2</sub>H<sub>6</sub> = 1712 ppmV is obtained when  $N_{\text{top}} = 7$  with Cr doping in this study.

## 1. Introduction

Due to mass consumption of fossil fuels, global warming and fossil fuels depletion have become a serious global environmental problem in the world. After the industrial revolution, the averaged concentration of CO<sub>2</sub> in the world has been increased from 280 ppmV to 387 ppmV by 2009. Therefore, it is necessary to develop a new energy production technology with less or no CO<sub>2</sub> emission.

It is reported that CO<sub>2</sub> can be reformed into fuels, for example, CO, CH<sub>4</sub>, CH<sub>3</sub>OH and H<sub>2</sub>, and so forth, by using TiO<sub>2</sub> as the photocatalyst under ultraviolet (UV) light illumination [1–10]. If this technique could be applied practically, a carbon circulation system would then be established: CO<sub>2</sub> from the combustion of fuel is reformed, using solar energy, to fuels again, and true zero emission can be achieved. Many R&D works on this technology have been carried out, using TiO<sub>2</sub> particles loaded with Cu, Pd, Pt to react with CO<sub>2</sub> dissolved in solution [1, 5, 7, 11–17]. Recently, nano-scaled TiO<sub>2</sub> [18–20], porous TiO<sub>2</sub> [21], TiO<sub>2</sub> film combined with

metal [22, 23], and dye-sensitized TiO<sub>2</sub> [24] are developed for this process. However, the fuel concentration in the products achieved in all the attempts so far is still low, ranging from 10 ppmV to 1000 ppmV, to be practically useful [1, 4, 5, 7, 8, 11, 12, 15, 16, 18, 20]. Therefore, the big breakthrough in increasing the concentration level is necessary to advance the CO<sub>2</sub> reforming technology.

In the applications such as water splitting and purification of pollutant, the photoresponse extension of TiO<sub>2</sub> to the visible spectrum has been investigated well [25–29]. TiO<sub>2</sub> by itself can only work under UV light due to its wide bandgap of 3.0–3.2 eV, which means that only about 4% of the incoming solar energy on the surface can be utilized [30]. On the other hand, the visible light accounts for 43% of whole solar energy [31]. Therefore, if the photoresponse of TiO<sub>2</sub> could be extended to the visible spectrum, the CO<sub>2</sub> reforming performance of TiO<sub>2</sub> technology would be improved significantly.

Doping with foreign ions is one of the most promising strategies for sensitizing TiO<sub>2</sub> to visible light and also for

forming charge traps to keep electron-hole pairs separate [32]. The most popular dopants for modification of the optical and photoelectrochemical properties of TiO<sub>2</sub> are transition metals such as Cr, Fe, Ni, V, Mn, and Cu [28]. Choi et al. [33] carried out a systematic investigation of the photocatalytic activity of TiO<sub>2</sub> doped with 21 different metal ions. It was found that doping with metal ions would introduce additional energy levels in the band gap of TiO<sub>2</sub> thus extending the photoresponse of TiO<sub>2</sub> into the visible spectrum. In addition, an optimum concentration of dopant metal ions exists under specific conditions. If the concentration of dopant exceeds the optimum one, the photocatalytic activity declines because of charge recombination [28]. Many previous reports on metal-doped TiO<sub>2</sub> used for photocatalytic degradation reaction of chemicals under visible light showed the activity enhancement only for a specific amount of doping ions, otherwise detrimental effects occur [34].

Many different techniques have previously been reported for metal doping of TiO<sub>2</sub> such as wet impregnation [35], hydrothermal deposition [36], RF magnetron sputtering deposition [24, 26, 37, 38], flame reactor method [39], solidstate reactions [40], ion implantation [41], and pulsed laser deposition [42]. Recently, the sol-gel method is adopted for metal doping of TiO<sub>2</sub> well [27–29, 34, 43–46] since this method can incorporate dopants into TiO<sub>2</sub> lattice, resulting in preparation of the materials with other optical and also catalytic properties [47]. In addition, the integration of dopants into the sol during the gelation process facilitates direct interaction with TiO<sub>2</sub> by sol-gel method [46].

Although many studies to extend the photoresponse of TiO<sub>2</sub> to the visible spectrum were reported as described above, there are only a few reports on its application for promoting the CO<sub>2</sub> reforming purposes [24]. In our previous studies [48–51], the effect of TiO<sub>2</sub> thin film preparation conditions in sol-gel and dip-coating process on the CO<sub>2</sub> reforming performance under UV light was investigated.

In this study, TiO<sub>2</sub> sol-gel and dip-coating process with doping is also adopted in order to extend its photoresponse to the visible spectrum to promote the CO<sub>2</sub> reforming performance. It was reported that the transition metals such as V, Cr, Mn, Fe, and Ni were effective for the photoresponse extension of TiO<sub>2</sub> to the visible spectrum [37]. According to the previous reports [28, 34, 39–41, 52, 53], it can be thought that Cr<sup>3+</sup> or Cr<sup>6+</sup> ion existing in TiO<sub>2</sub> film after doping can absorb the light of wavelength from 400 nm to 550 nm [28, 34, 39, 41, 52–55]. Therefore, Cr was selected at first as the dopant to check the feasibility of promoting CO<sub>2</sub> reforming performance of TiO<sub>2</sub> in this study. According to the study which investigated the photocatalytic H<sub>2</sub> evolution from water-alcohol mixtures, noble and base materials, including Pt, Au, Pd, Ni, Cu, and Ag, have been reported to be very efficient for increasing the production of H<sub>2</sub> by TiO<sub>2</sub> photocatalytic reaction [56]. According to the reaction scheme [1, 5, 6, 11, 16, 50, 51] of CO<sub>2</sub> reforming by TiO<sub>2</sub> photocatalyst as shown in Figure 1, if a lot of H<sup>+</sup> is produced, the reduction process is promoted, resulting in increase of the concentration of produced fuel. In addition, the photoresponse extension of TiO<sub>2</sub> to the visible spectrum

was obtained by Ni, Cu, and Ag doping in the previous study on the photocatalytic H<sub>2</sub> evolution from water-alcohol mixtures [56]. TiO<sub>2</sub> doped with Ag<sup>+</sup> ions absorbs the light of wavelength from 460 nm to 477 nm [56, 57]. Therefore, Ag was also selected at first as the dopant to check the feasibility of promoting CO<sub>2</sub> reforming performance of TiO<sub>2</sub> in this study.

In the present paper, the preparation method for doping Cr or Ag into TiO<sub>2</sub> film was developed. The characterization analyzed by scanning electron microscope (SEM), electron probe micro analyzer (EPMA), and X-ray photoelectron spectroscopy (XPS) was conducted. The influence of the ratio of amount of added Cr or Ag to amount of Ti in TiO<sub>2</sub> sol solution (*R*) and of the total coating number of Cr- or Ag-doped TiO<sub>2</sub> film (*N*) on CO<sub>2</sub> reforming characteristics under the condition of illuminating Xe lamp with or without UV light was also investigated in this study.

## 2. Experiment

**2.1. Preparation of Cr- or Ag-Doped TiO<sub>2</sub> Film.** Sol-gel and dip-coating process was used for preparing Cr- or Ag-doped TiO<sub>2</sub> film in this study. TiO<sub>2</sub> sol solution was made by mixing [(CH<sub>3</sub>)<sub>2</sub>CHO]<sub>4</sub>Ti (purity of 95 wt%, Nacalai Tesque Co.) of 0.1 mol, anhydrous C<sub>2</sub>H<sub>5</sub>OH (purity of 99.5 wt%, Nacalai Tesque Co.) of 0.8 mol, distilled water of 0.1 mol, and HCl (purity of 35 wt%, Nacalai Tesque Co.) of 0.008 mol. Cr powders (08819-15, Nacalai Tesque Co., particle size below 74 μm) or Ag powders (30934-92, Nacalai Tesque Co., particle size below 44 μm) were added into TiO<sub>2</sub> sol solution. Copper disc whose diameter and thickness were 50 mm and 1 mm, respectively, was dipped into Cr/TiO<sub>2</sub> or Ag/TiO<sub>2</sub> sol solution and pulled up at the fixed speed (*RS*) of 0.22 mm/s. Then, it was dried out and fired under the controlled firing temperature (*FT*) and firing duration time (*FD*), resulting in the fact that Cr- or Ag-doped TiO<sub>2</sub> film was fastened on the surface of copper disc. *FT* and *FD* was set at 623 K and 180 s, respectively. In this study, *N* varied from 1 to 7 for Cr doping and from 1 to 5 for Ag doping.

**2.2. Characterization of Cr- or Ag-Doped TiO<sub>2</sub> Film.** The surface structure and crystallization characteristics of Cr- or Ag-doped TiO<sub>2</sub> film were evaluated by SEM (JXA8900R, JEOL Ltd.) and EPMA (JXA8900R, JEOL Ltd.). The EPMA analysis helps us not only to understand the coating state of Cr- or Ag-doped TiO<sub>2</sub> on copper disc but also to measure the amount of doped Cr or Ag within TiO<sub>2</sub> film on copper disc. Element distribution through thickness direction of Cr-doped TiO<sub>2</sub> film was analysed by XPS (PHI Quantera SXM, ULVAC-PHI, INC.) using radiation source of Al radiation with the pass energy of 224.00 eV, the radiation current of 1.0 W, and the acceleration voltage of 15 kV.

**2.3. Apparatus and Procedure of CO<sub>2</sub> Reforming Experiment.** Figure 2 shows that the experimental system setup of CO<sub>2</sub> reformer consists of a stainless pipe (100 mm (*H.*)×50 mm (*I.D.*)), a copper disc (50 mm (*D.*)×1 mm (*t.*)) coated with Cr- or Ag-doped TiO<sub>2</sub> film which is located on the teflon

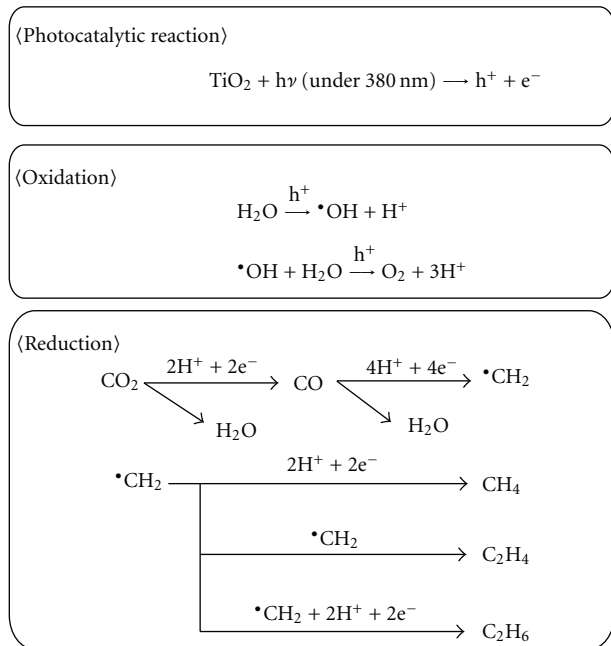


FIGURE 1: Reaction scheme of CO<sub>2</sub> reforming into fuel by TiO<sub>2</sub> photocatalyst (\*OH: hydroxy radical, \*CH<sub>2</sub>: carbon radical).

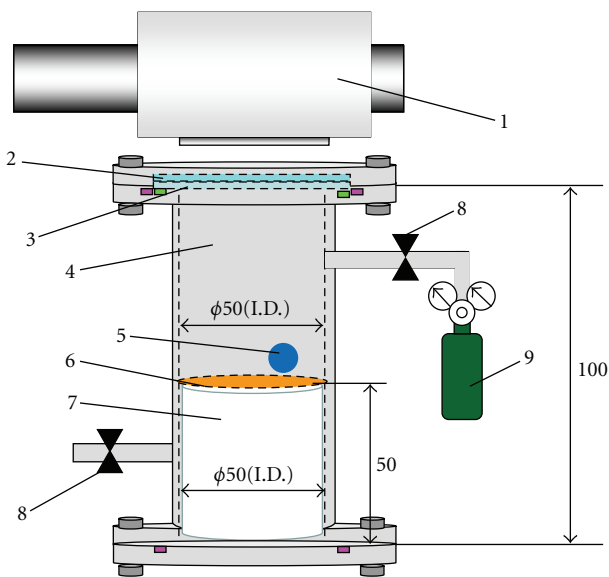


FIGURE 2: Schematic drawing of CO<sub>2</sub> reforming experimental system: ((1) Xe lamp; (2) coloured glass filter; (3) quartz glass disc; (4) stainless pipe; (5) gas sampling tap; (6) copper disc; (7) teflon cylinder; (8) valve; (9) CO<sub>2</sub> gas cylinder).

cylinder (50 mm (H.)×50 mm (D.)), a quartz glass disc (84 mm (D.)×10 mm (t.)), a coloured glass filter which cuts off the light of wavelength below 380 nm, SCF-50S-38L, SIGMA KOKI CO., LTD.), Xe lamp (L2175, Hamamatsu Photonics K. K.), and CO<sub>2</sub> gas cylinder. The reformer volume for CO<sub>2</sub> charge is 1.25×10<sup>-4</sup> m<sup>3</sup>. Xe lamp is located over the stainless pipe. The light of Xe lamp illuminates the copper disc coated with Cr- or Ag-doped TiO<sub>2</sub> film, which is inserted

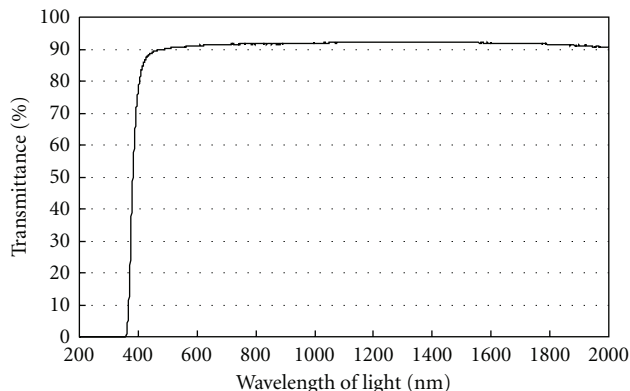


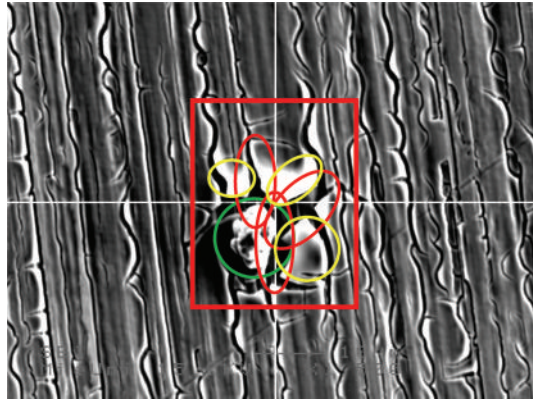
FIGURE 3: Light transmittance data of the coloured glass filter.

into the stainless pipe, through the coloured glass filter and the quartz glass disc fixed to the top of the stainless pipe. The wavelength of light from Xe lamp is ranged from 185 nm to 2000 nm. The Xe lamp can be fitted with a coloured glass filter to remove UV components of the light. With the filter, the wavelength of light from Xe lamp is ranged from 381 nm to 2000 nm. Figure 3 shows the light transmittance data of the coloured glass filter to prove the removal of the light whose wavelength is below 380 nm. The average light intensity of Xe lamp on the copper disc without and with setting the coloured glass filter is 57.53 mW/cm<sup>2</sup> and 43.67 mW/cm<sup>2</sup>, respectively.

In the CO<sub>2</sub> reforming experiment, CO<sub>2</sub> gas with the purity of 99.995 vol% was flowed through the CO<sub>2</sub> reformer as a purged gas for 15 minutes first. After that, the valves located at the inlet and the outlet of CO<sub>2</sub> reformer were closed. After confirming the gas pressure and gas temperature in the CO<sub>2</sub> reformer at 0.1 MPa and 298 K, respectively, the distilled water of 100 μL was injected into the CO<sub>2</sub> reformer, and Xe lamp illumination was turned on at the same time. The water injected vaporized completely in the reformer. Despite of the heat of UV lamp, the temperature in CO<sub>2</sub> reformer was kept at about 343 K during the CO<sub>2</sub> reforming experiment. The amount of injected water and that of CO<sub>2</sub> in CO<sub>2</sub> reformer was 5.56 mmol and 5.76 mmol, respectively. The gas in CO<sub>2</sub> reformer was sampled every 24 hours during the CO<sub>2</sub> reforming experiment. The gas samples were analyzed by FID gas chromatograph (GC353B, GL Science) and methanizer (MT221, GL Science). Minimum resolution of FID gas chromatograph and methanizer is 1 ppmV.

### 3. Results and Discussion

3.1. Analysis of Cr- or Ag-Doped TiO<sub>2</sub> Film by SEM and EPMA. Figures 4 and 5 show SEM image and EPMA image of Cr-doped TiO<sub>2</sub> film prepared under the condition of R = 1 wt%, respectively. Figures 6 and 7 show SEM and EPMA image of Ag-doped TiO<sub>2</sub> film prepared under the condition of R = 1 wt%, respectively. These SEM images were taken at 1500 times magnification under the condition of acceleration voltage of 15 kV and current of 3.0×10<sup>-8</sup> A. The red lined



— 10  $\mu\text{m}$   
 $\times 1500$

FIGURE 4: SEM images of Cr-doped  $\text{TiO}_2$  film prepared under the condition of  $R = 1$  wt%.

quadrangle area in Figures 4 and 6 was used for EPMA analysis shown in Figures 5 and 7, respectively. In Figures 5 and 7, the concentration of Ti, Cu, Cr, and Ag in observation area is indicated by the difference of colour. Light colours, for example, white, pink, and red indicate that the amount of element is large, while dark colours like black, blue, and green indicate that the amount of element is small.

The green circle in Figure 4 indicates the existence of Cr particle as shown in Figure 5. Moreover, the red circles illustrated in Figure 4 indicate that the amount of Cu is also large as pointed out by the white circles in Figure 5. On the other hand, the red circle in Figure 6 indicates the existence of Ag particle as shown in Figure 7. Furthermore, the yellow circles illustrated in Figure 6 indicate that the amount of Cu is small and Ti is large as pointed out by white circles in Figure 7. These results represent the following.

- (i) Before firing process,  $\text{Cr/TiO}_2$  or  $\text{Ag/TiO}_2$  sol solution is adhered on the copper disc uniformly.
- (ii) During firing process, the temperature profile of  $\text{Cr/TiO}_2$  or  $\text{Ag/TiO}_2$  sol solution adhered on the copper disc is not even due to the difference of thermal conductivity of Ti and Cr or Ag. Their thermal conductivity of Ti, Cr, and Ag at 600 K is 19.4 W/(m·K), 80.5 W/(m·K), and 405 W/(m·K), respectively [58]. Therefore, the thermal expansion around Cr or Ag particle and the thermal shrinkage around the other areas of  $\text{TiO}_2$  sol occur.
- (iii) Because of the thermal stress caused by the uneven distribution of temperature, the cluck around Cr or Ag and the shrinkage of  $\text{TiO}_2$  film around the cluck occur after firing process. Therefore, a large amount of Cu, which is an element of basis copper disc, around Cr or Ag and a large amount of Ti around Cr or Ag are observed in Figures 5 and 7.

To evaluate the amount of doped Cr or Ag within  $\text{TiO}_2$  film quantitatively, the observation area, which is the center of copper disc, of diameter of 300  $\mu\text{m}$  is analysed by EPMA.

The ratio of Cr or Ag to Ti in this observation area is counted by averaging the data obtained in this area.

Table 1 indicates the relationship between each element ratio and  $R$  which is varied from 1 wt% to 100 wt% when the  $N$  is set at 1 for Cr-doped  $\text{TiO}_2$  film. From this table, the ratio of Cr is increased with increasing  $R$  up to 70 wt% since the amount of Cr powders added into  $\text{TiO}_2$  sol solution is increased. However, the ratio of Cr starts to decrease if the  $R$  is over 70 wt%. The reason might be that when the amount of Cr powders in  $\text{TiO}_2$  sol solution was too much, the shrinkage of  $\text{TiO}_2$  film occurred. Therefore, the fixing strength of  $\text{TiO}_2$  film to copper disc was weakened, resulting in the ratio of Cr being decreased for  $R$  over 70 wt%. The ratio of Cr to Ti shown in Table 1, which is measured value, is different from the calculated  $R$  from the Cr powders added into  $\text{TiO}_2$  sol solution because of the agglomeration of Cr powders in  $\text{TiO}_2$  sol solution. Although Cr powders in  $\text{TiO}_2$  sol solution were mixed by magnetic stirrer well and the powders were stored under no moisture condition before the experiment, it was still difficult to prevent it from the agglomeration for such a fine particle completely.

Table 2 indicates the relationship between each element ratio and  $R$  which is varied from 1 wt% to 50 wt% when the  $N$  is set at 1 for Ag-doped  $\text{TiO}_2$  film. From this table, the ratio of Ag is increased with increasing  $R$  up to 50 wt% since the amount of Ag powders added into  $\text{TiO}_2$  sol solution is increased. However, the increase ratio of Ag is not so large compared to the exact amount of Ag powders added into  $\text{TiO}_2$  sol solution. The density of Ag which is 10787  $\text{kg/m}^3$  is much larger than the density of Ti which is 4507  $\text{kg/m}^3$ . Although  $\text{TiO}_2$  sol solution was mixed by magnetic stirrer well during dip-coating process, most of Ag particles were liable to sink in  $\text{TiO}_2$  sol solution in dip-coating process. Especially, for the case that  $R$  is over 10 wt%, the amount of Ag detected by EPMA is so small compared to the amount of Ag powders added into  $\text{TiO}_2$  sol solution, resulting in the fact that the control of doping a large amount of Ag by sol-gel and dip-coating process is quite difficult. The SEM image, that is, Figure 8, of Ag-doped  $\text{TiO}_2$  film prepared under the condition of  $R = 50$  wt% shows that there are many holes and clucks on  $\text{TiO}_2$  film, which are indicated by pink circles. However, fewer holes and clucks are seen in SEM image of Ag-doped  $\text{TiO}_2$  film prepared under the condition of  $R = 1$  wt% as shown in Figure 6. It is thought that these holes and clucks in Figure 8 are caused by peeling off  $\text{TiO}_2$  film. In addition, from EPMA image of Ag-doped  $\text{TiO}_2$  film prepared under the condition of  $R = 50$  wt% shown in Figure 9, it can be seen that there are some areas where the amount of Cu is large while the amount of Ti is small. These areas is pointed out by white circles, while Ag in surrounding areas are pointed out by red circles. This result is thought to be caused by peeling off  $\text{TiO}_2$  film around Ag particles. However, no such areas where the amount of Cu is large while the amount of Ti is small are observed in EPMA image of Ag-doped  $\text{TiO}_2$  film prepared under the condition of  $R = 1$  wt% as shown in Figure 7. Therefore, it can be concluded that the peeling off  $\text{TiO}_2$  film with Ag particles in dip-coating process only occurs under high  $R$  condition.

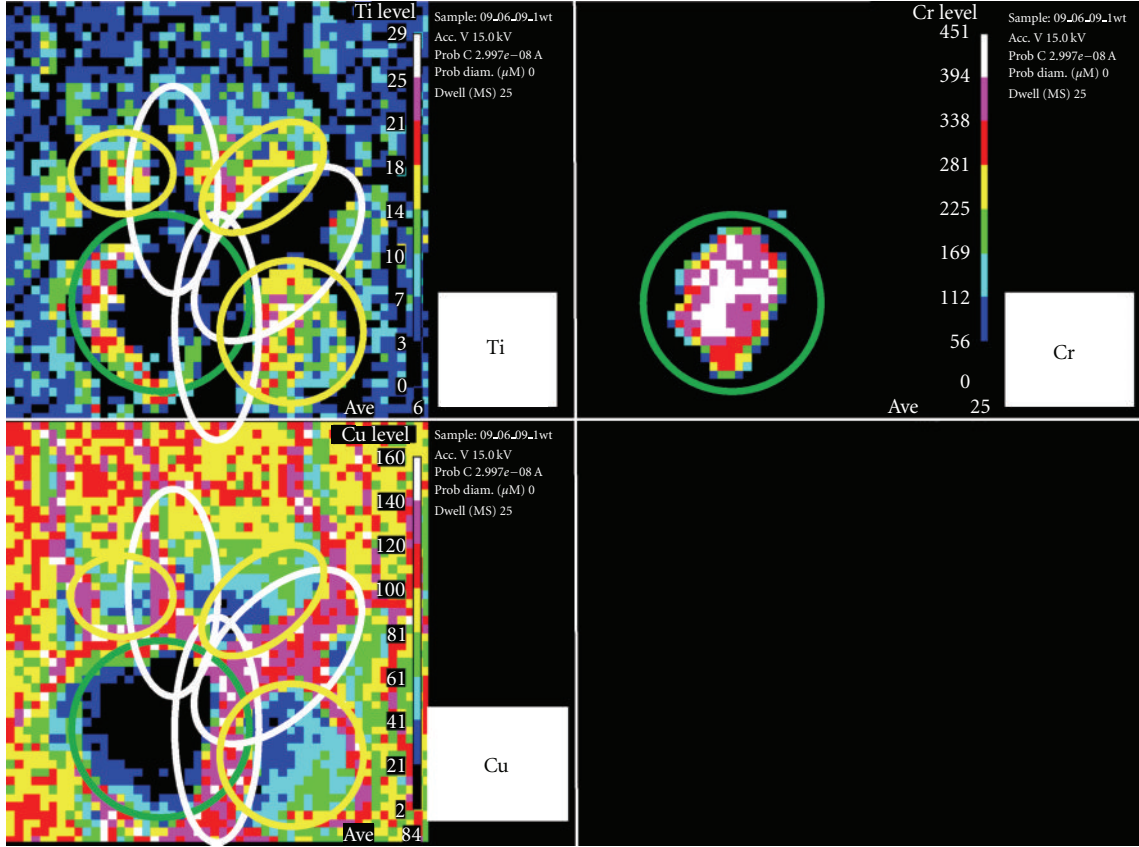


FIGURE 5: EPMA image of Cr-doped  $\text{TiO}_2$  film prepared under the condition of  $R = 1$  wt%.

TABLE 1: Relationship between each element and different  $R$  for Cr-doped  $\text{TiO}_2$  film.

$R$ [wt%]	1	10	20	30	40	50	60	70	80	90	100
Element											
Cr [wt%]	5.5	7.1	8.2	11.3	13.2	15.3	18.9	22.4	17.0	18.0	18.6
Ti [wt%]	94.5	92.9	91.8	88.7	86.8	84.7	81.1	77.6	83.0	82.0	81.4
Total	100.0	100.0	100.0	100.0	100.0	100.0	100.0	100.0	100.0	100.0	100.0

TABLE 2: Relationship between each element and different  $R$  for Ag-doped  $\text{TiO}_2$  film.

$R$ [wt%]	1	10	20	30	40	50
Element						
Ag [wt%]	0.6	1.4	1.9	2.5	2.6	3.4
Ti [wt%]	99.4	98.6	98.1	97.5	97.4	96.6
Total	100.0	100.0	100.0	100.0	100.0	100.0

### 3.2. Investigation of the Optimum Doping Ratio of Cr and Ag.

Figure 10 shows the concentration changes of CO produced by  $\text{CO}_2$  reforming along the time under the Xe lamp with UV light on, for several Cr- or Ag-doped  $\text{TiO}_2$  films prepared under the different  $R$  conditions. In this experiment, CO is the only fuel produced from  $\text{CO}_2$  reforming. Since the concentration of CO started to decrease after illumination of 72 hours for every  $R$ , Figure 10 only shows the concentration

up to 72 hours. Before this  $\text{CO}_2$  reforming experiment, a blank test, that is, running the  $\text{CO}_2$  reforming experiment without illumination of Xe lamp, has been carried out to set up a reference case. No fuel was produced in the blank test as expected.

According to Figure 10, the concentration of CO is increased with increasing  $R$  up to 70 wt% for Cr-doped  $\text{TiO}_2$  film. As Table 1 indicates that the ratio of Cr is also increased with increasing  $R$  up to 70 wt%, the result of  $\text{CO}_2$  reforming experiment matches well with the result of EPMA analysis. On the other hand, it is revealed that the concentration of CO for  $R = 1$  wt% which is larger than that for  $R = 50$  wt% though the amount of Ag detected by EPMA for  $R = 50$  wt% is larger than that for  $R = 1$  wt% as shown in Table 2. The reason to cause this result might be that  $\text{TiO}_2$  film was peeled off with Ag particles in dip-coating process especially under high  $R$  condition. Since the density of Ag is larger than that of Ti,  $\text{TiO}_2$  sol solution cannot keep Ag particles on copper disc



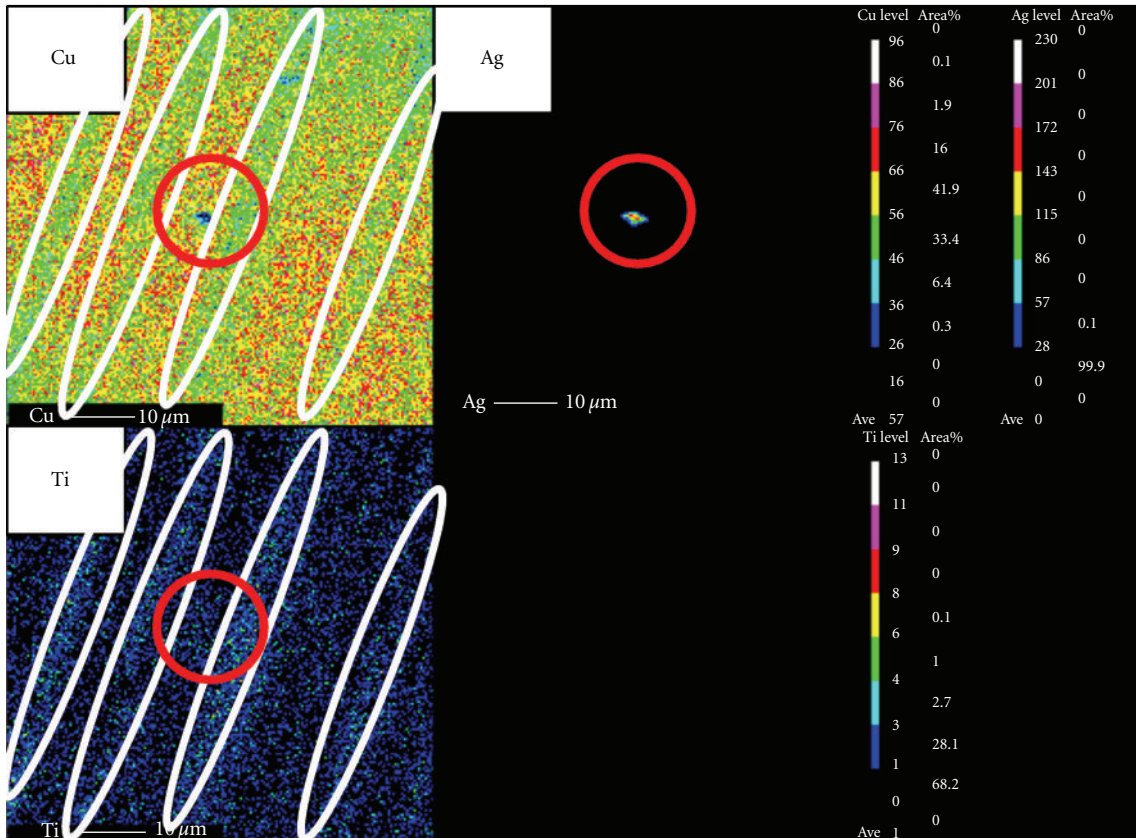
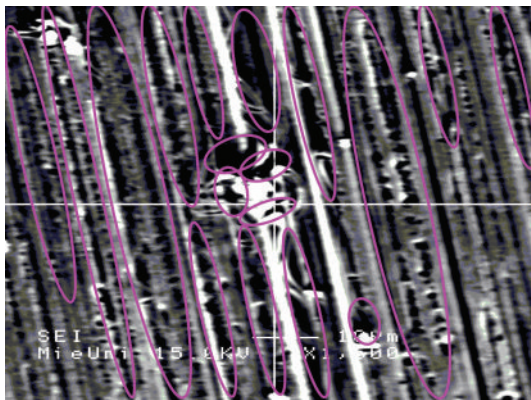


FIGURE 7: EPMA image of Ag-doped  $\text{TiO}_2$  film prepared under the condition of  $R = 1$  wt%.



— 10  $\mu\text{m}$   
 ×1500

FIGURE 8: SEM image of Ag-doped  $\text{TiO}_2$  film prepared under the condition of  $R = 50$  wt%.

the  $\text{CO}_2$  reforming performance of  $R = 50$  wt% is better than that of  $R = 1$  wt% if without UV light illumination, while the  $\text{CO}_2$  reforming performance of  $R = 1$  wt% is better than that of  $R = 50$  wt% if with UV light illumination. The  $\text{CO}_2$  reforming performance without UV light is generally lower than that with UV light irrespective of  $R$ . For example, when  $R = 50$  wt% after illumination of Xe lamp of 72 hours, the

$\text{CO}_2$  reforming performance without UV light is about thirty seventh part of that with UV light. The amount of Ag and the ratio of amount of  $\text{TiO}_2$  film to doped Ag are important to improve the photoresponse ability of doped  $\text{TiO}_2$  film, as shown in Figure 10. Therefore,  $R = 1$  wt% is selected as the optimum condition for Ag doping in this study as it gives the best result as shown in Figure 10. Another point to be noted is that, compared with Cr doping, Ag doping is much more effective to promote the  $\text{CO}_2$  reforming performance under the conditions with or without UV light.

**3.3. Effect of Coating Number of Cr- or Ag-Doped  $\text{TiO}_2$  Film on  $\text{CO}_2$  Reforming Characteristics.** Since the product of the  $\text{CO}_2$  reforming is only CO in this experiment, it is thought that the reduction effect of  $\text{TiO}_2$  is not so strong according to the reaction scheme shown in Figure 1. From Figure 1, more electron and proton are necessary to produce hydrocarbons like  $\text{CH}_4$ ,  $\text{C}_2\text{H}_4$ , and  $\text{C}_2\text{H}_6$ . When the reduction effect of  $\text{TiO}_2$  is promoted, the concentration of CO which is a pre-product to the hydrocarbons is also increased. The previous studies [48–51] show that the increase in  $N$  is effective to promote the reduction performance of  $\text{TiO}_2$  photocatalyst due to increase of the amount of  $\text{TiO}_2$ . Under the higher  $N$  condition, more electrons are produced by photocatalytic reaction. The effect of  $N$  of Cr- or Ag-doped  $\text{TiO}_2$  film on  $\text{CO}_2$  reforming performance and photoresponse ability of visible spectrum is investigated further below.

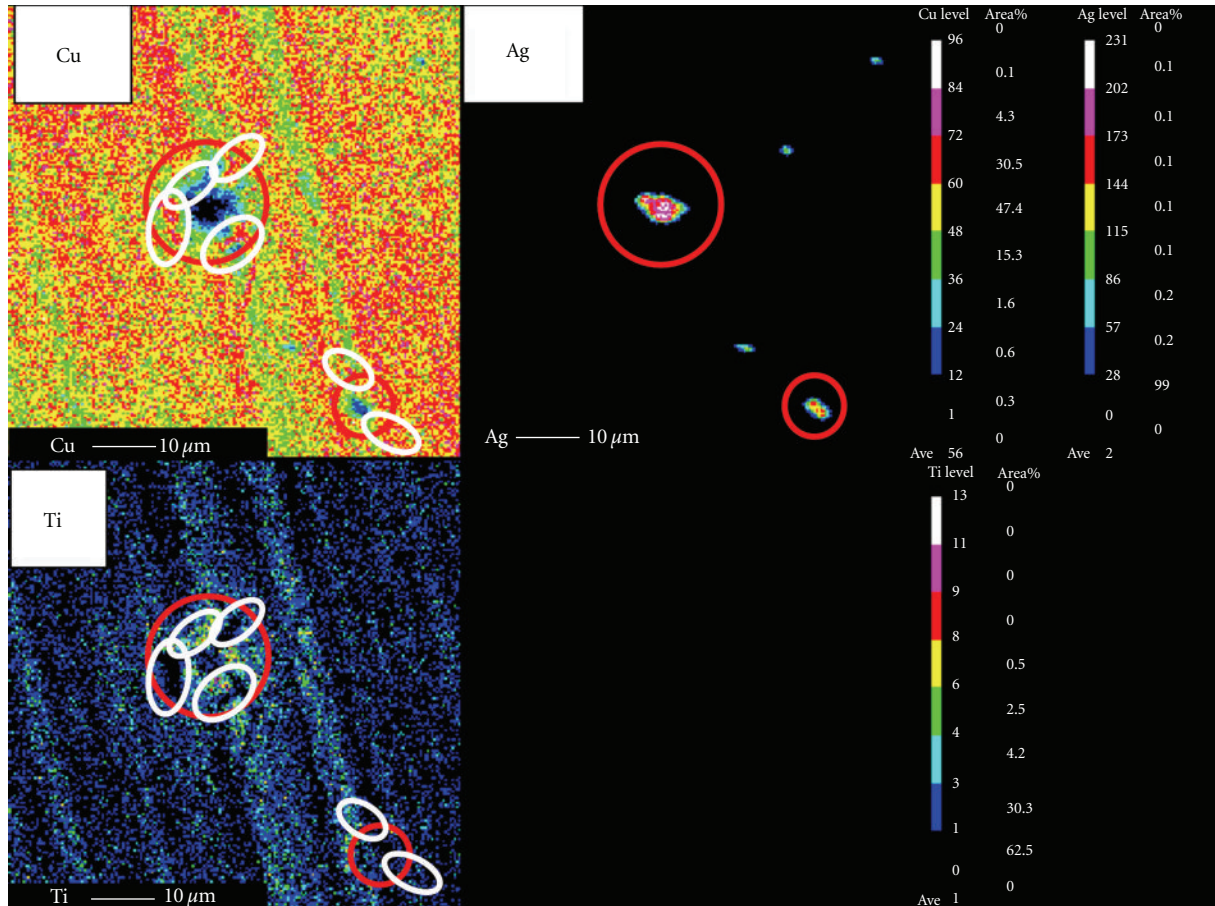


FIGURE 9: EPMA image of Ag-doped TiO<sub>2</sub> film prepared under the condition of  $R = 50$  wt%.

Figure 12 shows the concentrations of products from the CO<sub>2</sub> reforming after illumination of Xe lamp with UV light of 72 hours for several Cr-doped TiO<sub>2</sub> film prepared under conditions of different  $N$ . In this experiment, two coating conditions were investigated: Cr is doped in every layer ( $N_{\text{all}}$ ) and Cr is doped only in the top layer ( $N_{\text{top}}$ ), while  $R$  is fixed at 70 wt% in doping. Figure 12 indicates that the total concentration of products is increased with increasing  $N$ , since the amount of Cr-doped TiO<sub>2</sub> film coated on copper disc becomes larger with increasing  $N$ . However, the degree of the increase in  $N$  for  $N_{\text{top}}$  cases is higher than that for  $N_{\text{all}}$  cases. In addition, it is seen that CH<sub>4</sub> and C<sub>2</sub>H<sub>6</sub> as well as CO are produced more for  $N_{\text{top}}$  cases compared with  $N_{\text{all}}$  cases. This might be caused by the clucks occurring after finishing firing process. Each layer that is the base for next upper layer coating is weaker in  $N_{\text{all}}$  cases, resulting in the fact that the uniform coating for each layer is difficult to achieve. However, it is thought that the coating layers before the last coating are kept uniform in  $N_{\text{top}}$  cases. The reason why the concentrations of CH<sub>4</sub> and C<sub>2</sub>H<sub>6</sub> are increased with increasing  $N$  in  $N_{\text{top}}$  cases is thought to be the increase in the amount of TiO<sub>2</sub>.

Figure 13 shows the concentrations of products from CO<sub>2</sub> reforming after illumination of Xe lamp with UV light of 72 hours for several Ag-doped TiO<sub>2</sub> films prepared under

TABLE 3: Relationship between each element and different  $N$  for Ag-doped TiO<sub>2</sub> film.

$N$	$N_{\text{all}} = 1$	$N_{\text{all}} = 3$	$N_{\text{top}} = 3$	$N_{\text{top}} = 5$
Element				
Ag [wt%]	0.6	2.4	0.6	0.6
Ti [wt%]	99.4	97.6	99.4	99.4
Total	100.0	100.0	100.0	100.0

conditions of different  $N$ . In this experiment,  $R$  is fixed at 1 wt% in doping. And the results of  $N_{\text{all}}$  and  $N_{\text{top}}$  are shown in this figure. The data of other hydrocarbons, which were detected for every  $R$ , are omitted in this figure since the values of them are below 50 ppmV. From Figure 13, the best result is when  $N_{\text{all}} = 1$ , though EPMA analysis shown in Table 3 reveals that the largest amount of Ag detected is obtained when  $N_{\text{all}} = 3$  under the experimental conditions. When  $N$  is same, the ratio of detected Ag to total element for  $N_{\text{all}}$  is larger than that for  $N_{\text{top}}$ . Although a good promotion of CO<sub>2</sub> reforming performance was expected by EPMA analysis,  $N_{\text{all}} = 3$  does not show the good CO<sub>2</sub> reforming performance. In addition, the result of  $N_{\text{top}}$  is superior to the result of  $N_{\text{all}}$ . Under the condition of  $N_{\text{all}}$ , TiO<sub>2</sub> film is liable to be removed by increasing  $N$  since

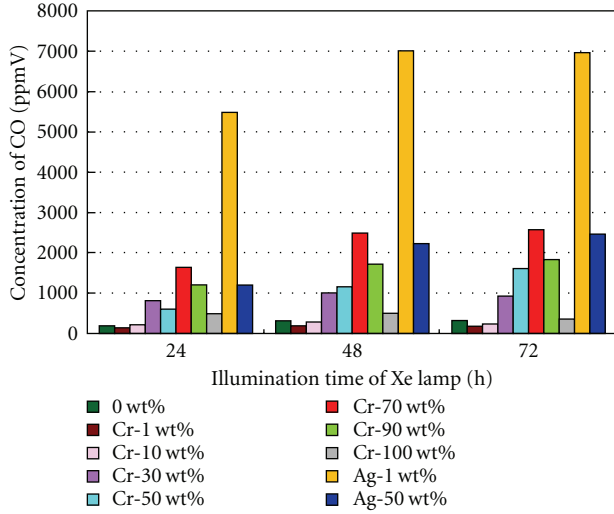


FIGURE 10: Comparison of produced concentration of CO among different  $R$  under the condition of illuminating Xe lamp with UV light.

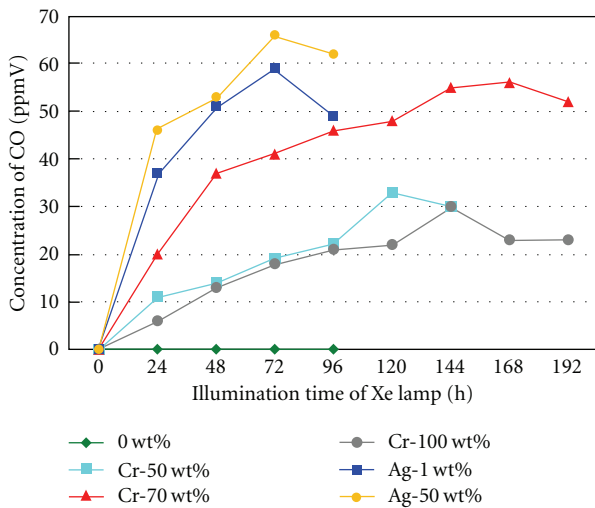


FIGURE 11: Comparison of produced concentration of CO among different  $R$  under the condition of illuminating Xe lamp without UV light.

doped Ag particles cause the uneven thin TiO<sub>2</sub> film on the former coated TiO<sub>2</sub> film and make TiO<sub>2</sub> film weak. Since Ag-doped TiO<sub>2</sub> film detaches, the amount of coated TiO<sub>2</sub> is decreased. On the other hand, under the condition of  $N_{top}$ , it is thought that even and steady thin TiO<sub>2</sub> film is coated more easily than  $N_{all}$ . Therefore, the CO<sub>2</sub> reforming performance of  $N_{top} = 3$  is better than that of  $N_{all} = 3$ . However, the CO<sub>2</sub> reforming performance of  $N_{top} = 5$  is worse compared with that of  $N_{top} = 3$ . It might be a result that doped Ag particles cause clucks of TiO<sub>2</sub> film during dip-coating process due to thermal stress. In the last coating, the former coated TiO<sub>2</sub> film under many  $N$  condition is weaker than that under small  $N$  condition, since the copper disc that is harder than TiO<sub>2</sub> film separates from the former

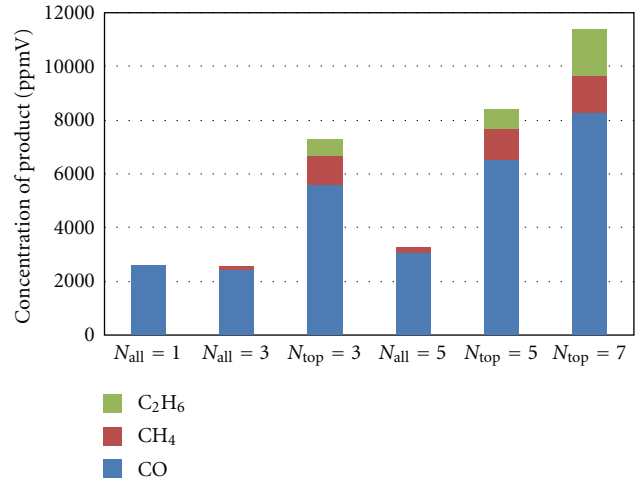


FIGURE 12: Comparison of product by CO<sub>2</sub> reforming after illumination of Xe lamp with UV light of 72 h for several Cr-doped TiO<sub>2</sub> film prepared under conditions of different  $N$ .

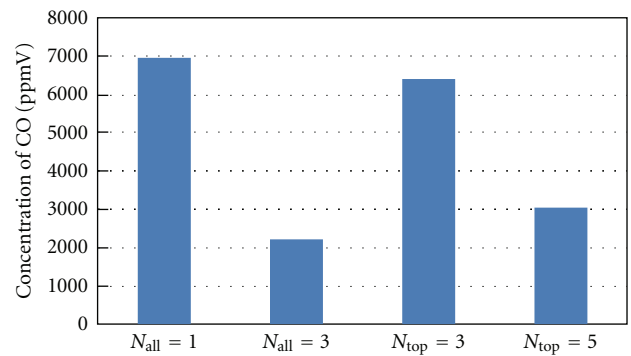


FIGURE 13: Comparison of product by CO<sub>2</sub> reforming after illumination of Xe lamp with UV light of 72 h for several Ag-doped TiO<sub>2</sub> film prepared under conditions of different  $N$ .

coated TiO<sub>2</sub> film by coating repetition. Therefore, the CO<sub>2</sub> reforming performance is worse with increasing  $N$  to 5. According to Figure 14 which shows the results without UV light, the CO<sub>2</sub> reforming performances of  $N_{top} = 3$  and  $N_{all} = 3$  are inferior to that of  $N_{all} = 1$ . Consequently, as to Ag doping, the  $N$  number seems having no impact on CO<sub>2</sub> reforming performance under both with and without UV conditions. Since the difference of thermal conductivities between Ag and Ti is larger than that between Cr and Ti, it is thought that the thermal stress becomes larger for Ag doping when  $N$  increases. By comparing all the results, the best CO<sub>2</sub> reforming was achieved under the condition of the  $N_{top} = 7$  with Cr doping in this study. Consequently, the large effect of many  $N$  on CO<sub>2</sub> reforming performance is obtained for Cr doping.

After illumination of Xe lamp with UV light of 72 hours, the concentration of CO, CH<sub>4</sub>, and C<sub>2</sub>H<sub>6</sub> can reach 8306 ppmV (= 92.5 mmol/g-catalyst), 1367 ppmV

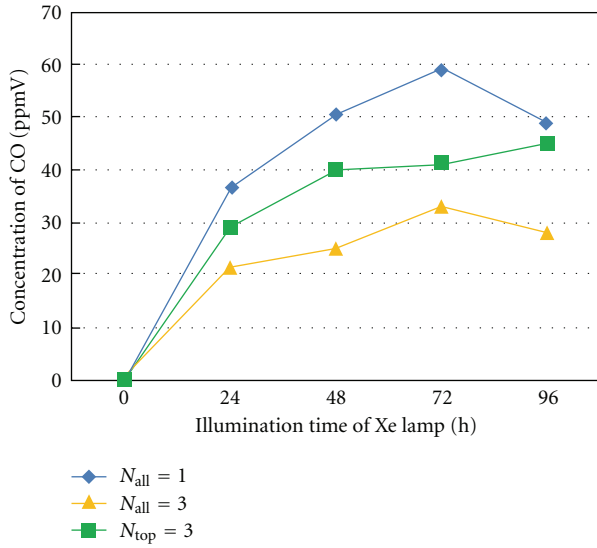


FIGURE 14: Comparison of concentration change of CO by CO<sub>2</sub> reforming with illumination time of Xe lamp without UV light for  $N_{all} = 1$ ,  $N_{all} = 3$  and  $N_{top} = 3$ .

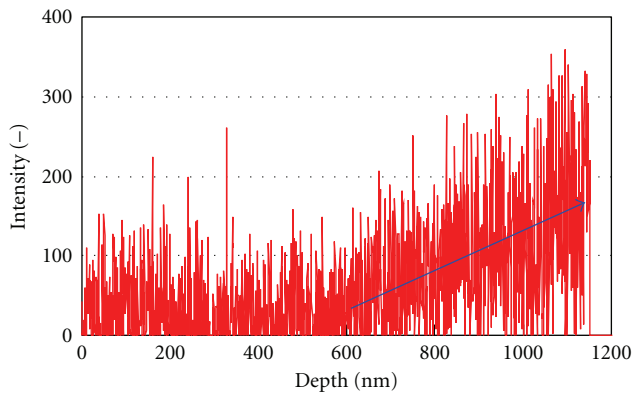


FIGURE 15: Cu element profile through thickness direction of the Cr-doped TiO<sub>2</sub> film under the condition of  $N_{top} = 7$  by XPS analysis.

(= 15.2 mmol/g-catalyst), and 1712 ppmV (= 19.1 mmol/g-catalyst), respectively, where the method to calculate the amount of product per weight of catalyst is as follows.

The thickness of Cr-doped TiO<sub>2</sub> film should be measured first, and then with the known surface area of copper disc of  $1.96 \times 10^{-3} \text{ m}^2$  and the density of TiO<sub>2</sub> of  $3900 \text{ kg/m}^3$  [60], the mass of TiO<sub>2</sub> can be calculated. XPS analysis was used to measure the thickness of Cr-doped TiO<sub>2</sub> film. Figure 15 shows the Cu element profile through thickness direction of the Cr-doped TiO<sub>2</sub> film in the case of  $N_{top} = 7$  by the XPS analysis. XPS spectra of Cu 3p are detected. In this XPS analysis, the sputtering rate is about 0.8 nm/min. It is seen that the intensity of Cu is increased dramatically from about 600 nm in this case. It alludes to the fact that the basis copper disc is at the depth of 600 nm; that is, the thickness of the TiO<sub>2</sub> film is 600 nm. In this calculation, the weight of Cr has been ignored since Cr was doped in the top layer only.

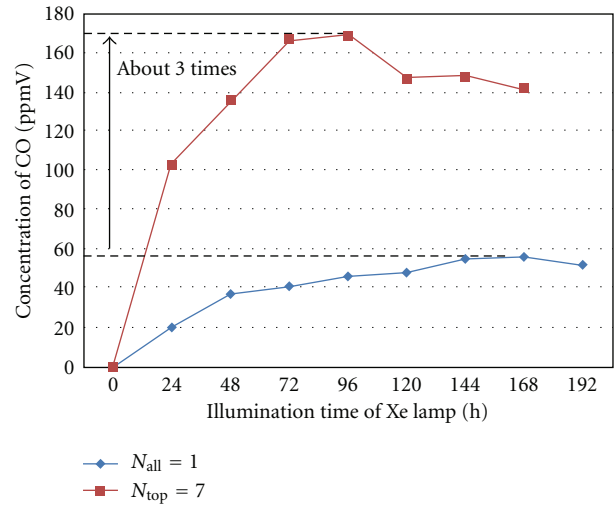


FIGURE 16: Comparison of concentration change of CO by CO<sub>2</sub> reforming with illumination time of Xe lamp without UV light for  $N_{all} = 7$  and  $N_{top} = 7$ .

To verify the effect of photoresponse extension of TiO<sub>2</sub> to the visible spectrum for  $N_{top} = 7$  in Cr coating, Figure 16 shows the results obtained with illumination time of Xe lamp without UV light. The data for  $N_{all} = 1$  under  $R = 70 \text{ wt}\%$  is also shown in this figure for comparison. Although CH<sub>4</sub> is produced from the experiment for  $N_{top} = 7$ , the concentration is below 10 ppmV. Therefore, Figure 16 shows the concentration of CO only. The peak value of concentration of CO for  $N_{top} = 7$  is about 3 times as large as that of  $N_{all} = 1$ . This proves that in the case of  $N_{top} = 7$ , the photoresponse ability of visible spectrum is also promoted by the increase of the amount of TiO<sub>2</sub> and the converted Cr ion-like Cr<sup>3+</sup> brought by encouragement of reduction performance of photocatalyst. Given that the concentration of product for  $R = 0 \text{ wt}\%$  is at such a low level as shown in Figures 10 and 11, it can be concluded that CO<sub>2</sub> reforming performance of TiO<sub>2</sub> is promoted dramatically by Cr doping. In the research by Ozcan et al. [24] which tried to extend the photoresponse of TiO<sub>2</sub> to the visible spectrum by Pt loading, the amount of product from CO<sub>2</sub> reforming without UV light was 104 times less than what we produced in this study. Therefore, Cr doping by sol-gel and dip-coating process is effective to promote the CO<sub>2</sub> reforming performance of TiO<sub>2</sub>.

#### 4. Conclusions

Based on the experimental results, the following conclusions can be drawn from this study.

Both Cr doping and Ag doping can promote the CO<sub>2</sub> reforming performance by TiO<sub>2</sub>. The optimum  $R$  when  $N = 1$  for Cr doping and Ag doping is 70 wt% and 1 wt%, respectively. Since the density of Ag is much larger than the density of Ti, the amount of Ag doped on TiO<sub>2</sub> film is lower compared to the actual amount of Ag powders added into TiO<sub>2</sub> sol solution, resulting in the fact that the good

CO<sub>2</sub> reforming performance is not obtained under large *R* condition. The promotion of CO<sub>2</sub> reforming performance by Cr or Ag doping comes from two aspects: (1) the photoresponse ability being extended to visible spectrum by the doping, and (2) doping preventing the recombination of electron and hole if there is UV light. The latter is stronger than the former. The best result obtained is in the case of  $N_{\text{top}} = 7$  with Cr doping under the investigated conditions in this study.

## Acknowledgment

The authors gratefully acknowledge the financial support from Tanikawa Fund Promotion of Thermal Technology.

## References

- [1] K. Adachi, K. Ohta, and T. Mizuno, "Photocatalytic reduction of carbon dioxide to hydrocarbon using copper-loaded titanium dioxide," *Solar Energy*, vol. 53, no. 2, pp. 187–190, 1994.
- [2] M. Anpo and K. Chiba, "Photocatalytic reduction of CO<sub>2</sub> on anchored titanium oxide catalysts," *Journal of Molecular Catalysis*, vol. 74, pp. 207–212, 1992.
- [3] B. Aurian-Blajeni, M. Halmann, and J. Manassen, "Photoreduction of carbon dioxide and water into formaldehyde and methanol on semiconductor materials," *Solar Energy*, vol. 25, no. 2, pp. 165–170, 1980.
- [4] G. R. Dey, A. D. Belapurkar, and K. Kishore, "Photo-catalytic reduction of carbon dioxide to methane using TiO<sub>2</sub> as suspension in water," *Journal of Photochemistry and Photobiology A*, vol. 163, no. 3, pp. 503–508, 2004.
- [5] K. Hirano, K. Inoue, and T. Yatsu, "Photocatalysed reduction of CO<sub>2</sub> in aqueous TiO<sub>2</sub> suspension mixed with copper powder," *Journal of Photochemistry and Photobiology A*, vol. 64, no. 2, pp. 255–258, 1992.
- [6] T. Inoue, A. Fujishima, S. Konishi, and K. Honda, "Photoelectrocatalytic reduction of carbon dioxide in aqueous suspensions of semiconductor powders," *Nature*, vol. 277, no. 5698, pp. 637–638, 1979.
- [7] O. Ishitani, C. Inoue, Y. Suzuki, and T. Ibusuki, "Photocatalytic reduction of carbon dioxide to methane and acetic acid by an aqueous suspension of metal-deposited TiO<sub>2</sub>," *Journal of Photochemistry and Photobiology A*, vol. 72, pp. 269–271, 1993.
- [8] S. Kaneco, H. Kurimoto, Y. Shimizu, K. Ohta, and T. Mizuno, "Photocatalytic reduction of CO<sub>2</sub> using TiO<sub>2</sub> powders in supercritical fluid CO<sub>2</sub>," *Energy*, vol. 24, no. 1, pp. 21–30, 1999.
- [9] K. Ogura, M. Kawano, J. Yano, and Y. Sakata, "Visible-light-assisted decomposition of H<sub>2</sub>O and photomethanation of CO<sub>2</sub> over CeO<sub>2</sub>-TiO<sub>2</sub> catalyst," *Journal of Photochemistry and Photobiology A*, vol. 66, no. 1, pp. 91–97, 1992.
- [10] K. Takeuchi, S. Murasawa, and T. Ibusuki, *World of Photocatalyst*, Kougyouchousakai, Tokyo, Japan, 2001.
- [11] Z. Goren, I. Willner, A. J. Nelson, and A. J. Frank, "Selective photoreduction of CO<sub>2</sub>/HCO<sub>3</sub><sup>-</sup> to formate by aqueous suspensions and colloids of Pd-TiO<sub>2</sub>," *Journal of Physical Chemistry*, vol. 94, no. 9, pp. 3784–3790, 1990.
- [12] M. Halmann, V. Katzir, E. Borgarello, and J. Kiwi, "Photoassisted carbon dioxide reduction on aqueous suspensions of titanium dioxide," *Solar Energy Materials*, vol. 10, no. 1, pp. 85–91, 1984.
- [13] T. Ibusuki, "Reduction of CO<sub>2</sub> by photocatalyst," *Syokubai*, vol. 35, pp. 506–512, 1993.
- [14] K. Kawano, T. Uehara, H. Kato, and K. Hirano, "Photocatalysed reduction of CO<sub>2</sub> in aqueous TiO<sub>2</sub> suspension mixed with various metal powder," *Kagaku to Kyoiku*, vol. 41, pp. 766–770, 1993.
- [15] C. C. Lo, C. H. Hung, C. S. Yuan, and J. F. Wu, "Photoreduction of carbon dioxide with H<sub>2</sub> and H<sub>2</sub>O over TiO<sub>2</sub> and ZrO<sub>2</sub> in a circulated photocatalytic reactor," *Solar Energy Materials and Solar Cells*, vol. 91, no. 19, pp. 1765–1774, 2007.
- [16] I. H. Tseng, W. C. Chang, and J. C. S. Wu, "Photoreduction of CO<sub>2</sub> using sol-gel derived titania and titania-supported copper catalysts," *Applied Catalysis B*, vol. 37, no. 1, pp. 37–48, 2002.
- [17] H. Yamashita, H. Nishiguchi, N. Kamada, and M. Anpo, "Photocatalytic reduction of CO<sub>2</sub> with H<sub>2</sub>O on TiO<sub>2</sub> and Cu/TiO<sub>2</sub> catalysts," *Research on Chemical Intermediates*, vol. 20, pp. 815–823, 1994.
- [18] P. Pathak, M. J. Mezziani, Y. Li, L. T. Cureton, and Y. P. Sun, "Improving photoreduction of CO<sub>2</sub> with homogeneously dispersed nanoscale TiO<sub>2</sub> catalysts," *Chemical Communications*, vol. 10, no. 10, pp. 1234–1235, 2004.
- [19] J. Qu, X. Zhang, Y. Wang, and C. Xie, "Electrochemical reduction of CO<sub>2</sub> on RuO<sub>2</sub>/TiO<sub>2</sub> nanotubes composite modified Pt electrode," *Electrochimica Acta*, vol. 50, no. 16–17, pp. 3576–3580, 2005.
- [20] X. H. Xia, Z. J. Jia, Y. Yu, Y. Liang, Z. Wang, and L. L. Ma, "Preparation of multi-walled carbon nanotube supported TiO<sub>2</sub> and its photocatalytic activity in the reduction of CO<sub>2</sub> with H<sub>2</sub>O," *Carbon*, vol. 45, no. 4, pp. 717–721, 2007.
- [21] F. Cecchet, M. Alebbi, C. A. Bignozzi, and F. Paolucci, "Efficiency enhancement of the electrocatalytic reduction of CO<sub>2</sub>: *fac*-[Re(*v*-bpy)(CO)<sub>3</sub>Cl] electropolymerized onto mesoporous TiO<sub>2</sub> electrodes," *Inorganica Chimica Acta*, vol. 359, no. 12, pp. 3871–3874, 2006.
- [22] L. F. Cueto, G. A. Hirata, and E. M. Sánchez, "Thin-film TiO<sub>2</sub> electrode surface characterization upon CO<sub>2</sub> reduction processes," *Journal of Sol-Gel Science and Technology*, vol. 37, no. 2, pp. 105–109, 2006.
- [23] J. C. S. Wu and H. M. Lin, "Photo reduction of CO<sub>2</sub> to methanol via TiO<sub>2</sub> photocatalyst," *International Journal of Photoenergy*, vol. 7, no. 3, pp. 115–119, 2005.
- [24] O. Ozcan, F. Yukruk, E. U. Akkaya, and D. Uner, "Dye sensitized CO<sub>2</sub> reduction over pure and platinumized TiO<sub>2</sub>," *Topics in Catalysis*, vol. 44, no. 4, pp. 523–528, 2007.
- [25] M. Kitano, M. Matsuoka, M. Ueshima, and M. Anpo, "Recent developments in titanium oxide-based photocatalysts," *Applied Catalysis A*, vol. 325, no. 1, pp. 1–14, 2007.
- [26] M. Kitano, M. Takeuchi, M. Matsuoka, J. M. Thomas, and M. Anpo, "Photocatalytic water splitting using Pt-loaded visible light-responsive TiO<sub>2</sub> thin film photocatalysts," *Catalysis Today*, vol. 120, no. 2, pp. 133–138, 2007.
- [27] X. Yang, C. Cao, K. Hohn et al., "Highly visible-light active C- and V-doped TiO<sub>2</sub> for degradation of acetaldehyde," *Journal of Catalysis*, vol. 252, no. 2, pp. 296–302, 2007.
- [28] R. Dholam, N. Patel, M. Adami, and A. Miotello, "Hydrogen production by photocatalytic water-splitting using Cr- or Fe-doped TiO<sub>2</sub> composite thin films photocatalyst," *International Journal of Hydrogen Energy*, vol. 34, no. 13, pp. 5337–5346, 2009.
- [29] T. Kamegawa, J. Sonoda, K. Sugimura, K. Mori, and H. Yamashita, "Degradation of isobutanol diluted in water over visible light sensitive vanadium doped TiO<sub>2</sub> photocatalyst," *Journal of Alloys and Compounds*, vol. 486, no. 1–2, pp. 685–688, 2009.
- [30] Y. Xie, Q. Zhao, X. J. Zhao, and Y. Li, "Low temperature preparation and characterization of N-doped and N-S-codoped

- TiO<sub>2</sub> by sol-gel route,” *Catalysis Letters*, vol. 118, no. 3-4, pp. 231–237, 2007.
- [31] D. Li, N. Ohashi, S. Hishita, T. Kolodiazny, and H. Haneda, “Origin of visible-light-driven photocatalysis: a comparative study on N/F-doped and N-F-codoped TiO<sub>2</sub> powders by means of experimental characterizations and theoretical calculations,” *Journal of Solid State Chemistry*, vol. 178, no. 11, pp. 3293–3302, 2005.
- [32] A. Fujishima, X. Zhang, and D. A. Tryk, “TiO<sub>2</sub> photocatalysis and related surface phenomena,” *Surface Science Reports*, vol. 63, no. 12, pp. 515–582, 2008.
- [33] W. Choi, A. Termin, and M. R. Hoffmann, “The role of metal ion dopants in quantum-sized TiO<sub>2</sub>: correlation between photoreactivity and charge carrier recombination dynamics,” *Journal of Physical Chemistry*, vol. 98, no. 51, pp. 13669–13679, 1994.
- [34] J. Zhu, Z. Deng, F. Chen et al., “Hydrothermal doping method for preparation of Cr<sup>3+</sup>-TiO<sub>2</sub> photocatalysts with concentration gradient distribution of Cr<sup>3+</sup>,” *Applied Catalysis B*, vol. 62, no. 3-4, pp. 329–335, 2006.
- [35] J. A. Navio, G. Colon, M. I. Litter, and G. N. Bianco, “Synthesis, characterization and photocatalytic properties of ion-doped titanium semiconductors prepared from TiO<sub>2</sub> and iron (III) acetylacetonate,” *Journal of Molecular Catalysis A*, vol. 106, no. 3, pp. 267–276, 1996.
- [36] J. Zhu, W. Zheng, B. He, J. Zhang, and M. Anpo, “Characterization of Fe-TiO<sub>2</sub> photocatalysts synthesized by hydrothermal method and their photocatalytic reactivity for photodegradation of XRG dye diluted in water,” *Journal of Molecular Catalysis A*, vol. 216, no. 1, pp. 35–43, 2004.
- [37] M. Anpo, “Preparation, characterization, and reactivities of highly functional titanium oxide-based photocatalysts able to operate under UV-visible light irradiation: approaches in realizing high efficiency in the use of visible light,” *Bulletin of the Chemical Society of Japan*, vol. 77, no. 8, pp. 1427–1442, 2004.
- [38] M. Anpo and M. Takeuchi, “The design and development of highly reactive titanium oxide photocatalysts operating under visible light irradiation,” *Journal of Catalysis*, vol. 216, no. 1-2, pp. 505–516, 2003.
- [39] J.-M. Herrmann, J. Disdier, and P. Pichat, “Effect of chromium doping on the electrical and catalytic properties of powder titania under UV and visible illumination,” *Chemical Physics Letters*, vol. 108, no. 6, pp. 618–622, 1984.
- [40] H. Kato and A. Kudo, “Visible-light-response and photocatalytic activities of TiO<sub>2</sub> and SrTiO<sub>3</sub> photocatalysts codoped with antimony and chromium,” *Journal of Physical Chemistry B*, vol. 106, no. 19, pp. 5029–5034, 2002.
- [41] M. Anpo, M. Takeuchi, K. Ikeue, and S. Dohshi, “Design and development of titanium oxide photocatalysts operating under visible and UV light irradiation. The applications of metal ion-implantation techniques to semiconducting TiO<sub>2</sub> and Ti/zeolite catalysts,” *Current Opinion in Solid State and Materials Science*, vol. 6, no. 5, pp. 381–388, 2002.
- [42] T. Sumita, T. Yamaki, S. Yamamoto, and A. Miyashita, “Photo-induced surface charge separation in Cr-implanted TiO<sub>2</sub> thin film,” *Thin Solid Films*, vol. 416, no. 1-2, pp. 80–84, 2002.
- [43] X. Yang, C. Cao, L. Erickson, K. Hohn, R. Maghirang, and K. Klabunde, “Photo-catalytic degradation of Rhodamine B on C-, S-, N-, and Fe-doped TiO<sub>2</sub> under visible-light irradiation,” *Applied Catalysis B*, vol. 91, no. 3-4, pp. 657–662, 2009.
- [44] W. S. Tung and W. A. Daoud, “New approach toward nanosized ferrous ferric oxide and Fe<sub>3</sub>O<sub>4</sub>-doped titanium dioxide photocatalysts,” *Applied Materials & Interfaces*, vol. 1, pp. 2453–2461, 2009.
- [45] J. Xu, Y. Ao, and D. Fu, “A novel Ce, C-codoped TiO<sub>2</sub> nanoparticles and its photocatalytic activity under visible light,” *Applied Surface Science*, vol. 256, no. 3, pp. 884–888, 2009.
- [46] H. Žabová and V. Čírkva, “Microwave photocatalysis III. Transition metal ion-doped TiO<sub>2</sub> thin films on mercury electrodeless discharge lamps: preparation, characterization and their effect on the photocatalytic degradation of monochloroacetic acid and Rhodamine B,” *Journal of Chemical Technology and Biotechnology*, vol. 84, no. 11, pp. 1624–1630, 2009.
- [47] M. Subramanian, S. Vijayalakshmi, S. Venkataraj, and R. Jayavel, “Effect of cobalt doping on the structural and optical properties of TiO<sub>2</sub> films prepared by sol-gel process,” *Thin Solid Films*, vol. 516, no. 12, pp. 3776–3782, 2008.
- [48] A. Nishimura, N. Sugiura, S. Kato, N. Maruyama, and S. Kato, “High yield CO<sub>2</sub> conversion into CH<sub>4</sub> by photocatalyst multilayer film,” in *Proceedings of the 2nd International Energy Conversion Engineering Conference*, pp. 824–832, AIAA2004-5619, August 2004.
- [49] A. Nishimura, N. Sugiura, M. Fujita, S. Kato, and S. Kato, “Influence of photocatalyst film forming conditions on CO<sub>2</sub> reforming,” in *Proceedings of the 3rd International Energy Conversion Engineering Conference*, pp. 248–257, AIAA2005-5536, August 2005.
- [50] A. Nishimura, N. Sugiura, M. Fujita, S. Kato, and S. Kato, “Influence of preparation conditions of coated TiO<sub>2</sub> film on CO<sub>2</sub> reforming performance,” *Kagaku Kogaku Ronbunshu*, vol. 33, no. 2, pp. 146–153, 2007.
- [51] A. Nishimura, M. Fujita, S. Kato, and S. Kato, “CO<sub>2</sub> reforming performance of coated TiO<sub>2</sub> film with supported metal,” *Kagaku Kogaku Ronbunshu*, vol. 33, no. 5, pp. 432–438, 2007.
- [52] C. C. Pan and J. C. S. Wu, “Visible-light response Cr-doped TiO<sub>2</sub>-xNx photocatalysts,” *Materials Chemistry and Physics*, vol. 100, no. 1, pp. 102–107, 2006.
- [53] S. W. Bae, P. H. Borse, S. J. Hong et al., “Photophysical properties of nanosized metal-doped TiO<sub>2</sub> photocatalyst working under visible light,” *Journal of the Korean Physical Society*, vol. 51, no. 1, pp. S22–S26, 2007.
- [54] M. Anpo, “Photocatalysis on titanium oxide catalysts—approaches in achieving highly efficient reactions and realizing the use of visible light,” *Catalysis Surveys from Japan*, vol. 1, no. 2, pp. 169–179, 1997.
- [55] B. Sun, E. P. Reddy, and P. G. Smirniotis, “Effect of the Cr<sup>6+</sup> concentration in Cr-incorporated TiO<sub>2</sub>-loaded MCM-41 catalysts for visible light photocatalysis,” *Applied Catalysis B*, vol. 57, no. 2, pp. 139–149, 2005.
- [56] A. V. Kozhakov, N. I. Ermokhina, A. L. Stroyuk et al., “Photocatalytic hydrogen evolution over mesoporous TiO<sub>2</sub>/metal nanocomposites,” *Journal of Photochemistry and Photobiology A*, vol. 198, no. 2-3, pp. 126–134, 2008.
- [57] E. A. Streltsov, R. M. Lazorenko-Manevich, V. P. Pakhomov, and A. I. Kulak, “Surface states formed on titanium dioxide by deposition of copper,” *Electrochemistry*, vol. 19, p. 1148, 1983.
- [58] Japan Society of Mechanical Engineering, *Heat Transfer Handbook*, Maruzen, Tokyo, Japan, 1st edition, 1993.
- [59] A. Nishimura, N. Komatsu, G. Mitsui, M. Hirota, and E. Hu, “CO<sub>2</sub> reforming into fuel using TiO<sub>2</sub> photocatalyst and gas separation membrane,” *Catalysis Today*, vol. 148, no. 3-4, pp. 341–349, 2009.
- [60] Y. Nosaka and A. Nosaka, *Introduction of Photocatalyst*, Tokyotosho, Tokyo, Japan, 1st edition, 2004.

